"Melting Transition" of a Quantum Dot Solid: Collective Interactions Influence the Thermally-Induced Order−Disorder Transition of a Silver Nanocrystal Superlattice

Brian A. Korgel,*,† Nelsi Zaccheroni,‡ and Donald Fitzmaurice‡

Department of Chemical Engineering, and the Texas Materials Institute University of Texas Austin, Texas 78712-1062
Department of Chemistry, University College Dublin Belfield, Dublin 4 Ireland

Received July 23, 1998

Creating materials with physical properties that differ from those found in nature has long been a scientific goal. One approach is to use organic-monolayer stabilized nanocrystals (<100 Å in diameter) as building blocks to construct artificial solids.[1−3] When the size distribution is sufficiently narrow, simply by evaporating the solvent from a concentrated dispersion a "quantum dot solid" can be formed.[3] Relatively little is known about the thermal stability of these new materials; however, collective *mesoscopic* interactions between particles might be expected to effect unique phase behavior.

This study examined the thermal stability of a face-centered cubic (fcc) dodecanethiol-capped silver nanocrystal superlattice (Figure 1) using simultaneous small-angle X-ray scattering (SAXS) and differential scanning calorimetry (DSC).[4,5] Structural rearrangements with angstrom resolution were measured as a function of temperature, along with the associated enthalpic changes. The SAXS data reveals many qualitative signatures of a true melting transition (Figure 2d). However, the DSC data indicates broad second-order behavior, similar to order−disorder transitions in alloys.

Silver quantum dot solids were formed by evaporating 200 μL of dodecanethiol-capped silver nanocrystals dispersed hexane (5 mg/mL) on a mica substrate at room temperature. These thin film superlattices exhibit long range order (Figures 1 and 2).[4] Superlattices formed using the same nanocrystals exhibit consistently reproducible *d* spacing and superlattice structure, supporting the fact that these films represent true relaxed equilibrium structures, similar to superlattice "crystallites".[1] Simultaneous DSC and SAXS measurements (Figure 2) were performed on beam line 8.2 of the Synchrotron Radiation Source (SRS) at the Daresbury Laboratory, Warrington, U.K.,[3] using a specially designed DSC sample holder (Linkham THM).[3−5] The static structure factor $S(q)$, was used to calculate the radial distribution function $g(r)$, which represents the probability of finding another particle at a distance r from the origin of a central particle (Figure 3a).[4,7]

Between 30 and 140 °C, temperature has little effect on the fcc structure of the quantum dot solid, and the SAXS pattern (Figure 2a) remains relatively unchanged. The intensity I_T and position q_{max} of the diffraction peaks, however, decrease slightly

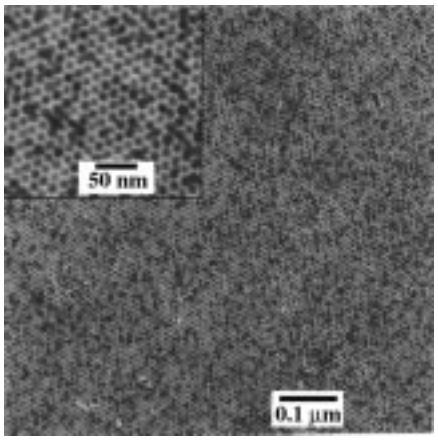

Figure 1. TEM image: dodecanethiol-capped silver nanocrystals with a core radius of 35 ± 2.5 Å on a carbon substrate.

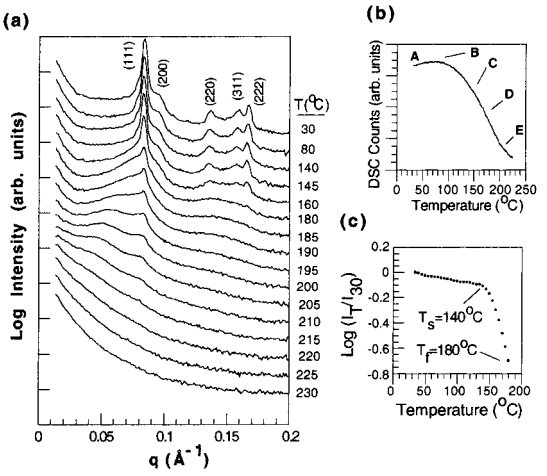

(d)

Temperature (°C)	DSC transition	Structural behavior
<75	A	reversible lattice expansion
75-140	B	irreversible lattice expansion
140-180	C	mode **I**—pre-melting transition; enhanced vibrations accompanied by bare nanocrystal dimerization
180-210	D	mode **II**—disordering of monolayer-stabilized nanocrystals
210-230	E	mode **III**—bare nanocrystal clustering

Figure 2. Simultaneous SAXS/DSC data obtained for the silver quantum dot solid. (a) Temperature-dependent SAXS diffraction patterns with (b) the corresponding DSC data. Points A (30−75 °C), B (75 °C), C and D (determined to be 140 and 180 °C from the SAXS data, respectively), and E (205 °C), label transitions in the DSC data. (c) Effective Debye−Waller plot of for the (111) diffraction peak versus temperature. (d) Summary table.

* To whom correspondence should be addressed.
† University of Texas at Austin.
‡ University College Dublin.

(1) Murray, C. B.; Kagan, C. R.; Bawendi, M. G. *Science* **1995**, *270*, 1335−1338.
(2) Korgel, B. A.; Fitzmaurice, D. *Phys. Rev. Lett.* **1998**, *80*, 3531−3534.
(3) Korgel, B. A.; Fullam, S.; Connolly, S.; Fitzmaurice, D. *J. Phys. Chem. B* **1998**, *102*, 8379−8388; Korgel, B. A.; Fitzmaurice, D. *Phys. Rev. B*, in press.

(4) Silver nanocrystals were prepared by organic-phase reduction in the presence of dodecanethiol ($C_{12}H_{25}SH$) with subsequent size-selective precipitation with chloroform/ethanol as the solvent/nonsolvent pair to obtain a narrow size distribution.[7] Several superlattices were formed with the same silver nanocrystal sample and tested to ensure reproducibility of the transition temperatures. A ^{1}H NMR spectrum of the nanocrystals in chloroform-*d* confirmed that all of the dodecanethiol present in solution was adsorbed at the silver nanocrystal surface, and FTIR spectroscopy and elemental analysis confirmed that the thiol headgroups are close-packed on the nanocrystal surface.[3] SAXS patterns of the quantum dot solid indexed to an fcc solid with a d_{111} spacing of 75.3 Å, which corresponds to an interparticle separation δ_{SL}, of 17 Å. The data presented represents a typical experiment. The DSC scan rate was tested, and 5 °C/min was sufficiently slow to eliminate any apparent kinetic effects. The SAXS data was collected in one minute frames. The scattering intensity $I(q)$ (where $q = (4\pi/\lambda) \sin\theta$ with θ as the scattering angle 2θ, and $\lambda = 1.54$ Å) relates proportionally to the shape factor $P(qR)$ and the static structure factor $S(q)$: $I(q) \propto P(qR)S(q)$.[8] $P(qR)$ was measured first for hexane-dispersed nanocrystals to calculate $S(q)$ during melting.[3,8]

(5) Bras, W.; Derbyshire, G. E.; Devine, A.; Clark, S. M.; Cooke, J.; Komanschek, B. E.; Ryan, A. J. *J. Appl. Crystallogr.* **1995**, *28*, 26−32.

10.1021/ja9826035 CCC: $18.00
Published on Web 03/25/1999

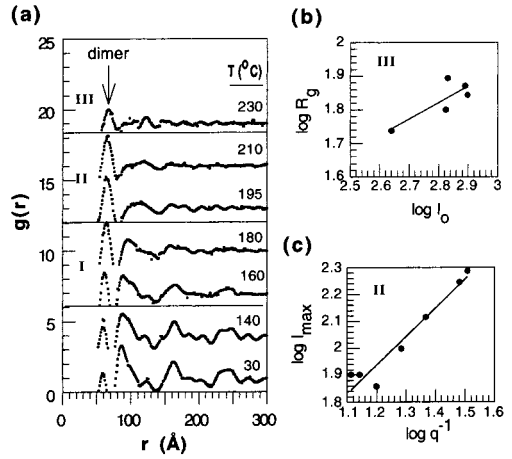

Figure 3. (a) SAXS data in Figure 2a transformed to $g(r)$. (b) $I_{o,T}/I_{o,\ 210\ °C}$ plotted versus R_g for mode **III** to determine exponent m of the relation, $I_{o,T}/I_{o,\ 210\ °C} \propto R_g^m$. (c) I_T versus q_{max} plotted for mode **II**. Values of $m = 0.05$ and $n = 1$are consistent with the growth of concentration fluctuations during both modes.[14,15]

with increasing temperature. To understand this behavior, I_T was plotted versus temperature in Figure 2c. The slope M is related to the vibrational mean square displacement $\langle u \rangle$ of the nanocrystals in the superlattice and the interparticle spacing d: $M = -0.5 \ln (I_T/I_o) = \langle u \rangle^2/d^2$.[6] For a single phase, M is expected to remain constant.[6] Raising the temperature from 30 to 140 °C increases δ_{SL} by 2 Å, which corresponds to an expansion coefficient for the superlattice of $\alpha_{SL} = (1/v)(dV/dT)_p = 6.6 \times 10^{-4}\ ^0K^{-1}$.[9] By assuming negligible expansion of the silver cores compared to the chains and using the measured value of α_{SL}, α_{chain} equals a typical value for liquid hydrocarbons ($\alpha_{chain} = 1.2 \times 10^{-3}\ ^0K^{-1}$). The capping ligands expand the quantum dot solid. Interestingly, dodecanethiol melts at 18 °C—well below 140 °C—yet the superlattice does not lose its structural integrity.

The superlattice expansion could be cycled reversibly between 70 °C and temperatures at least as low as −50 °C, repeatedly. However, once the temperature reached 75 °C and greater, the superlattice no longer contracted with decreased temperature. The DSC measurements in Figure 2b reveal a broad endothermic transition (B) at 75 °C, which most likely corresponds to thiol ligand desorption off the particle surface.[10] Therefore, thiol desorption appears to affect the reversibility of the superlattice expansion, however, below 140 °C the nanocrystals remain ordered in an fcc structure. The free energy gained by ordering exceeds any structural perturbations created by thiol desorption.

The SAXS data reveal a distinct phase transition at 140 °C. The vibrational displacement in the superlattice increases dramatically (Figure 2c). Between 140 and 180 °C, $g(r)$ reveals that the interparticle spacing and positional distribution increase; however, the majority of particles do not leave their lattice positions. The behavior in this temperature range can be interpreted as a premelting transition (mode **I**).[11]

Further examination of $g(r)$ during mode **I** reveals that a minority of bare nanocrystals dimerize. In the room-temperature superlattice, a perceptible amount of silver core dimers already exist (see Figure 3a and Figure 1); however, the dimer concentration remains constant up to 140 °C. Above this temperature $\langle u \rangle$ greatly increases (Figure 2c), consequently bringing a much greater number of silver core surfaces close enough to induce irreversible aggregation. This structural transition correlates with a broad enthalpic change in the DSC data (C in Figure 2b).

At 180 °C, the second to fifth order (inclusive) diffraction peaks disappear with the loss of long range order (denoted as mode **II**). The density profile exhibits oscillations characteristic of fluid structure. $S(q)$ for the first-order diffraction peak decreases from 3.5 to 2.5 as the temperature increases from 180 to 185 °C, which is consistent with the Hansen−Verlet criteria for melting where $S(q) = 2.85$.[12] The DSC data, however, suggests a continuous second-order endothermic transition (D).[8,9]

During mode **II**, $g(r)$ changes little with increased temperature. Further dimerization does not occur, possibly due to the stress relief provided by disordering.[6] A shoulder appears at the low-q side of the (111) diffraction peak in Figure 2a and shifts to lower q with increasing temperature, indicating the growth of a new scattering domain. The dimensionality n, of the growing domains can be determined: the intensity I, of the low-q diffraction feature and q_{max} are related by $I \propto q^n$.[15] From the values plotted in Figure 3c, $n = 1$, which is consistent with spinodal decomposition of the ordered nanocrystal phase.[14]

Above 210 °C, a third mode of disordering appears. The low-q diffraction feature present during mode **II** disappears, but the slope of the scattering curve at low q continues to increase. The radius of gyration R_g, of the scatterers at 210 °C was determined to be 55 Å from the slope of the scattering curve at low q using the Guinier approximation, $I/I_o = \exp(-q^2R_g/3)$).[8] These "domains" are too large to be attributed to individual nanocrystals. As the temperature increases above 210 °C, R_g and I_o continue to increase and $g(r)$ changes dramatically. At 230 °C, the short-range order between organic-monolayer coated particles prevalent during mode **II**, disappears, with a high probability of finding bare particles with surfaces touching. The plot of $I_{o,T}/I_{o,\ 210\ °C}$ versus R_g for temperatures above 210 °C in Figure 3b, reveals that the scattering domains grow as concentration fluctuations—consistent with *a phase separation* between bare silver particles and hydrocarbons.[14] Since the temperature is less than the boiling point of dodecanethiol (280 °C), significant hydrocarbon evaporation is unlikely. An enthalpic transition also appears in the DSC data ((E) in Figure 2b). Mode **III** can be interpreted as a rearrangement and aggregation of silver cores within a liquid hydrocarbon phase.

In summary, a continuous second-order melting (or disordering) transition has been observed at 180 °C, with an associated premelting transition at 140 °C. These transition temperatures do not correlate with the melting, conformational, desorption, or boiling temperatures of dodecanethiol. Therefore, it appears that the cohesive attractions between nanocrystals and collective entropy gained by ordering contributes a substantial amount of stabilization energy to the superlattice.

Acknowledgment. The authors thank Dr. E. Komanschek at the Central Laboratory of the Research Councils, Daresbury and the Commission of the European Union for funding through the Large Scale Facilities Program.

JA9826035

(6) Ubbelohde, A. R. *The Molten State of Matter*: John Wiley & Sons: New York, 1978.

(7) $g(r)$ was calculated using $S(q)$ and the nanocrystal number density ρ:[7].

$$g(r) = 1 + \frac{1}{2\pi^2\rho r}\int q(S(q) - 1)\sin(qr)dq \qquad (1)$$

(8) Glatter, O.; Kratky, O. Eds. *Small-Angle X-ray Scattering*: Academic Press: New York, 1982.

(9) West, A. R. *Solid State Chemistry and its Applications*: John Wiley & Sons: New York, 1984.

(10) Leff, D. V.; Brandt, L.; Heath, J. R. *Langmuir* **1996**, *12*, 4723−4730.

(11) Mode **I** could be interpreted as an *fcc* → *bcc* transition: characteristic of *bcc* packing with eight nearest neighbors and six next nearest neighbors, the nearest neighbor peak in $g(r)$ has split slightly;[13] and during an *fcc* → *bcc* transition $\langle u \rangle^2$ will also become significantly enhanced.[8]

(12) Hansen, J. P.; Verlet, L. *J. Chem. Phys.* **1969**, *184*, 151.

(13) Robbins, M. O.; Kremer, K.; Grest, G. S. *J. Chem. Phys.* **1988**, *88*, 3286−3312.

(14) Cumming, A.; Wiltzius, P.; Bates, F. S.; Rosedale, J. H. *Phys. Rev. A* **1992**, *45*, 885−897.

(15) de Gennes, P. G. *Scaling Concepts in Polymer Physics*: Cornell University Press: Ithaca, New York, 1979.